Optimization of the luminescence emission of Si nanocrystals synthesized from non-stoichiometric Si oxides using a Central Composite Design of the deposition process

B. Morana , J.C.G. de Sande , A. Rodríguez , J. Sangrador ,
T. Rodríguez , M. Avella , J. Jiménez

Dpto. Tecnología Electrónica, E.T.S.I. de Telecomunicación, Universidad Politécnica de Madrid, 28040 Madrid, Spain
Dpto. Ingeniería de Circuitos y Sistemas, E.U.I.T. de Telecomunicación, Universidad Politécnica de Madrid, 28031 Madrid, Spain
Dpto. Física de la Materia Condensada, E.T.S.I. Industriales, Universidad de Valladolid, 47011 Valladolid, Spain

Abstract

Si oxide films with a controlled excess of Si were deposited on Si wafers by LPCVD using Si_2H_6 and O_2, thermally annealed to 1100 °C for 1 h to form Si nanocrystals embedded in SiO_2 and subsequently annealed at 450 °C in forming gas. The samples were characterized by Fourier transform infrared spectroscopy, spectroscopic ellipsometry and cathodoluminescence spectroscopy. The excess of Si in the as-deposited samples, ranging from 0 to 70% in volume, was obtained from the ellipsometry data analysis. After annealing at 1100 °C, the samples show a luminescence band (peaking at 665 nm) at 80 K and at room temperature which is associated to the presence of Si nanocrystals. The growth rate, the excess of Si incorporated to the films and the intensity of the luminescence band were modelled using a Face-Centered Central Composite Design as a function of the main deposition variables (pressure, 185–300 mTorr; temperature, 250–400 °C; Si_2H_6/O_2 flow ratio, 2–5) aiming to control the growth process and the incorporation of Si in excess as well as to determine the experimental conditions that yield the samples with the maximum intensity of the luminescence emission.

Keywords: Non-stoichiometric Si oxides; Si nanocrystals; Face-Centered Central Composite Design; FTIR spectroscopy; Spectroscopic ellipsometry; Cathodoluminescence

1. Introduction

Si nanocrystals embedded in SiO_2 obtained by precipitation of the excess of Si in non-stoichiometric silicon oxide films may be obtained using different techniques In this work, the non-stoichiometric oxide layers have been deposited using a Low Pressure Chemical Vapor Deposition (LPCVD) reactor. The as-deposited samples were characterized by Fourier transform infrared (FTIR) spectroscopy and spectroscopic ellipsometry (SE) to determine their composition, thickness and refractive index. The effect of the post-growth annealing processes has been studied using cathodoluminescence spectroscopy (CL). To find the experimental conditions to achieve a sufficiently slow growth rate to control the thickness of the films, a controlled amount of Si incorporated in excess and the maximum intensity of the luminescence emission, the system has been characterized using a Face-Centered Central Composite Design (FCCD)

2. Experimental

2.1. Samples preparation

The deposition was carried out on Si wafers using a LPCVD deposition system with Si_2H_6 and O_2 as precursor gases and N_2 as carrier gas. The process parameters were selected based on our previous results on the deposition of stoichiometric oxides The pressure was varied between 185 and 300 mTorr and the temperature between 250 and 450 °C. The Si_2H_6/O_2 gas flow ratio was varied between 2 and 5 to ensure that the gas is

rich enough in the precursor of Si. The total flow was 102 sccm, being 90 sccm the flow of N_2 in all the experiments and 12 sccm the total flow of the reactant species, which was kept constant.

The as-deposited samples were annealed in a furnace at 1100 °C for 1 h to segregate the Si in excess. An additional treatment was performed in H_2–N_2 at 450 °C for 1 h.

The volume fraction occupied by the excess (E) of Si incorporated into the deposited layers and the growth rate (V) of the as-deposited layers as well as the intensity (I) of the luminescence emission in the annealed samples were modeled as a function of the process temperature (T), pressure (P) and Si_2H_6/O_2 flow ratio (R) using a FCCD The coded values of the main variables ranging from −1 (lowest value) to +1 (highest value) were used for the analysis. The 17 experiments necessary for the full characterization of the system as a function of the three variables (T, R, P) are the eight vertices (±1, ±1, ±1), the central points of the six faces (±1, 0, 0), (0, ±1, 0) and (0, 0, ±1) as well as three repetitions of the central point of the cube (0, 0, 0) to analyze the reproducibility of the process. The significance of the different effects of the variables (mains, linear interactions between them and quadratic terms) was determined. The data were analyzed using the Design-Expert® 7.1.1 Software [6]. The results obtained for the 17 points corresponding to the full experiment are used in all cases to generate constant value contour graphs of the magnitudes of interest as a function of the most relevant variables.

2.2. *Characterization techniques*

The composition of the samples was analyzed using a Perkin-Elmer Spectrum 100 FTIR spectrometer in the 200–7800 cm^{-1} wavenumber range. The absorbance spectra were normalized to the layer thickness yielding the absorption coefficient spectra.

The thickness (t), the refractive index (n) and the volume fraction of the excess of Si in the layers were determined from SE measurements carried out in the 270–1200 nm wavelength range for incidence angles of 70°, 75°, and 80° using a variable angle rotating analyzer ellipsometer (J.A. Woollam Co., Inc.). To interpret the measurements, several fitting procedures have been used. First, a Cauchy function dependence of the n on the wavelength has been assumed in the long wavelength spectral range, where the film absorption is almost zero, and n and t have been determined with no further assumptions on the nature of the material. Once t is known, the method also yields n and the extinction coefficient for shorter wavelengths. Then, the volume fraction of Si in excess has been estimated using an Effective Medium Approximation (EMA) of a mixture of SiO_2 and amorphous Si to represent the optical properties of the layer (E and t are taken now as fitting parameters). For small values of E (below 5%), it has been found that Maxwell–Garnett and Bruggeman EMA give almost the same results, and the values of t obtained differ less than 1 nm, in films around 100 nm thick, from those determined previously using the Cauchy function. The value of t is used as a test for the validity of the results. For values of E higher than 5%, the Bruggeman EMA fits more properly the optical properties of the film than the Maxwell–Garnett EMA Also, the values of t derived from the fittings are in better agreement with those determined previously using the Cauchy function when Bruggeman EMA rather than Maxwell–Garnett EMA is used. In these cases, however, the obtained value of E can only be considered as an estimation of the actual value since a mixture of SiO_2 and amorphous Si may not be an adequate representation of the structure of the film when the excess of Si is so high. The growth rate (V) was calculated as the ratio between t and the deposition time.

The annealed and as-deposited samples were characterized by cathodoluminescence spectroscopy. The CL emission was measured at 80 K and at room temperature using a XiCLOne system (Gatan) attached to a SEM (JEOL 820) operating with an e-beam acceleration voltage of 5 kV and a beam current of 10 nA. To compare the intensities of the different emissions taking into account the total amount of Si in excess available for the formation of nanocrystals in the different samples, the acquired CL spectra were divided by the corresponding as-deposited layer thickness. After the appropriate background removal, the bands of interest were extracted from the spectra and their areas were calculated. The values of these areas were divided by the maximum one to yield the normalized intensities.

3. Results

3.1. *As-deposited samples: deposition process*

Fig. 1 shows a selected region of the absorption coefficient spectra obtained by FTIR spectroscopy of several as-deposited layers with different volume fractions of Si in excess. The spectra show the three bands characteristic of SiO_2, which are located at 450, 810 and 1080 cm^{-1}, but shifted from these positions, and other absorption bands in the 700–900 cm^{-1} wavenumber range. Absorption bands at 700, 850 and 875 cm^{-1} have been previously attributed to the bending mode of Si–H bonds [9], and a band located at 870 cm^{-1} has been attributed to the SiH_2 scissors vibration [10]. Both effects, the shift of the peaks and the existence of bands associated to the presence of H, point to

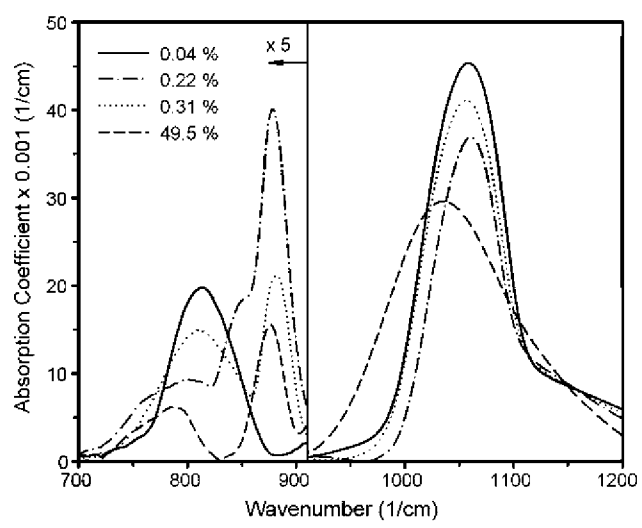

Fig. 1. Absorption coefficient spectra of selected as-deposited samples with different Si contents.

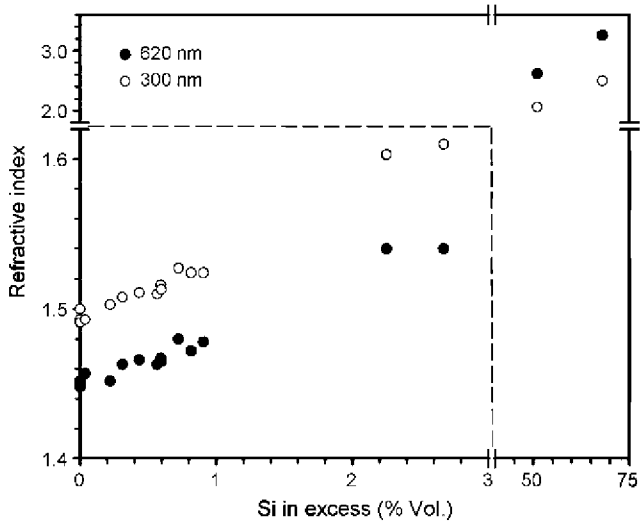

Fig. 2. Refractive index at 620 and 300 nm of the as-deposited samples as a function of the Si content.

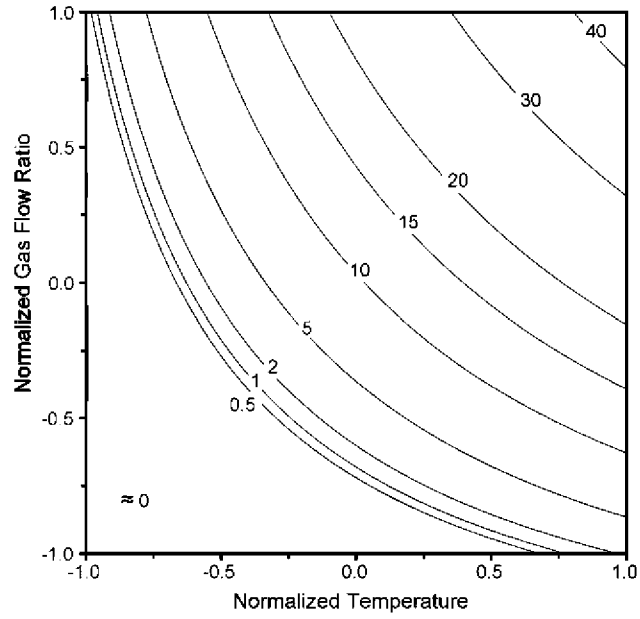

Fig. 3. Excess of Si, E (% Si vol.), as a function of the normalized values of T and R at $P=+1$.

the non-stoichiometry of the as-deposited oxides. The intensity of peaks related with H decreases as the deposition temperature increases, due to the enhancement of the hydrogen desorption.

Fig. 2 shows n at two different wavelengths (300 and 620 nm) determined using the fitting procedure based on the Cauchy function as a function of the volume fraction of Si in excess obtained using the Bruggeman EMA fitting method. The better quality of the fittings obtained using the Bruggeman EMA instead of the Maxwell–Garnett EMA throughout the whole range of values of E (from 0 to near 70%) suggests that the as-deposited films are homogeneous in nature, rather than a matrix with randomly located inclusions or clusters. The growth rates, in the 15–60 nm/h interval, are appropriate for the controlled deposition of layers with thickness from 10 nm to several tens of nm in a reasonable process time.

Figs. 3 and 4 summarize the main results of the FCCD experiment concerning the deposition process. The excess of incorporated Si depends significantly on the temperature ($\sim T$) and on the gas flow ratio ($\sim R$), being noticeable the importance of the effect of the interaction between them ($\sim T \times R$), which reinforces the incorporation of Si to the films when both variables take high values. The model for the growth rate includes significant effects of the temperature ($\sim T$), the temperature squared ($\sim T^2$), the gas flow ratio ($\sim R$) and the interaction between the temperature and the gas flow ratio ($\sim T \times R$). The effect of the pressure is not statistically significant in any case. The graphs included in Figs. 3 and 4, are representative of the results obtained for all values of P. The analysis indicates that the models described above for E and V are significant, with a chance below 0.05% that the observed results could occur due to noise. However, the model for the excess of Si shows a lack of fit, i.e. the fraction of the total error which cannot be explained in terms of errors in the reproducibility of the process. Two possible causes related with the ellipsometric data analysis may be considered: the H incorporated to the films, which influence has not been taken into account in the fittings, and the use of an EMA of a mixture of SiO_2 and amorphous Si, which may be considered inadequate for samples with a high amount of Si in excess. With regard to the incorporation of H, Fig. 1 shows that in the samples deposited at low temperatures, which are those that incorporate a small or moderate excess of Si, the areas of the Si–H absorption bands are the highest ones. However, in these cases the fittings of the ellipsometric data using the EMA of a mixture of SiO_2 and Si are excellent, indicating that the influence of hydrogen on the optical properties of the films may be considered negligible. Therefore, the use of a model based on a mixture of SiO_2 and amorphous Si, which may not be an appropriate representation of the structure of the samples with

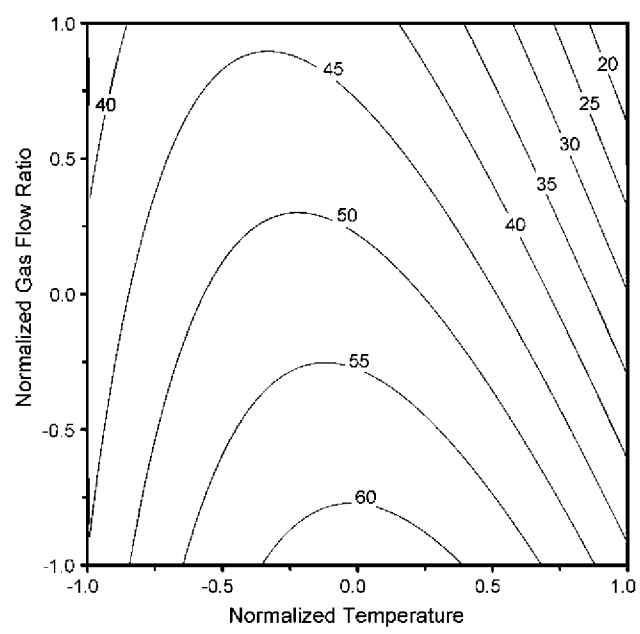

Fig. 4. Growth rate, V (nm/h), as a function of the normalized values of T and R at $P=+1$.

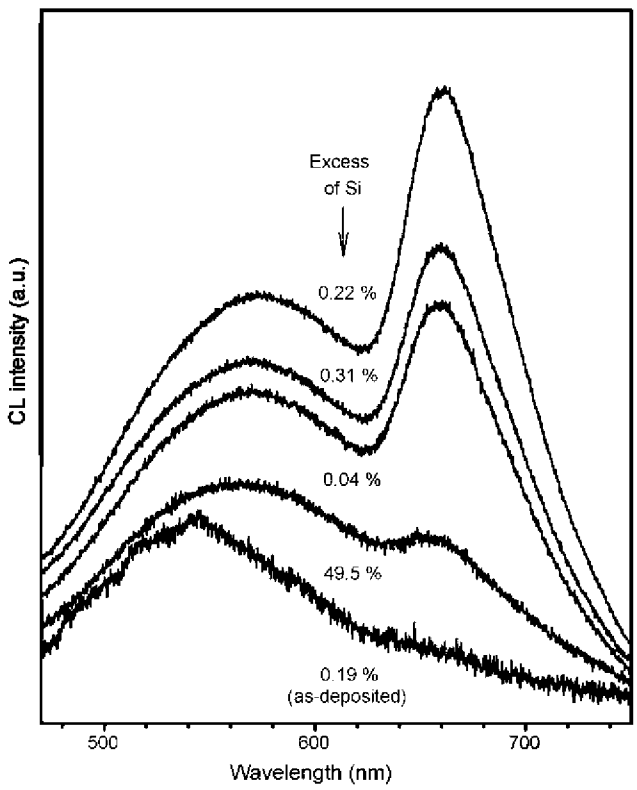

Fig. 5. CL spectra of annealed samples with layers of different Si contents and a spectrum of an as-deposited sample.

a high excess of Si, appears as the most probable cause for the lack of fit observed following the FCCD analysis.

The results presented in Figs. 3 and 4 are in close correlation to each other. At the $(-1, -1, P)$ region, for the minimum values of the temperature and the flow ratio, the amount of Si in excess incorporated to the layers is very small, so the deposited material is almost pure SiO_2. If R is increased while keeping T constant, a slight and progressive increase in E takes place, reaching values of around 0.25% at $(-1, +1, P)$, and the growth rate decreases due to the progressive incorporation of Si to the films. If T is increased keeping R constant, the incorporation of Si in excess to the films is more noticeable than in the previous case, reaching values close to 2.5% at $(+1, -1, P)$. The oxide growth rate first increases due to the effect of the increase in the temperature and then decreases since the deposited layer is incorporating a substantial amount of Si. The main effect of the interaction between the temperature and the gas flow ratio is to reinforce the decrease of the growth rate at high values of both variables, being noticeable the low values obtained near the $(+1, +1, P)$ edge compared to those in other regions.

3.2. *Annealed samples: luminescence emission*

The CL spectra of several annealed samples and an as-deposited one are displayed in Fig. 5. The spectra show two major broad luminescence bands. One of them is present in the spectra of both the as-deposited and annealed samples. After annealing, this band is broadened and its position shifted to around 570 nm in all samples. It is associated in the literature to the SiO_2 matrix The other band, present only in the annealed samples, is associated to the presence of the Si nanoparticles formed during the annealing process. Its peak position, 665 nm, does not depend on the deposition parameters, and therefore on the size of the nanoparticles. This result rules out any influence of quantum confinement on the luminescence emission and suggests that it arises from recombination at defects located at the Si nanoparticles/SiO_2 matrix interface, whose energy is insensitive to the crystal size.

Fig. 6 displays the main results of the FCCD modelling of the normalized intensity (I) of the 665 nm luminescence band. This graph is representative of the behaviour observed for all values of P. These results are in close correlation with those of the excess of Si included in Fig. 3. Near the $(-1, -1, P)$ edge, where the excess of Si incorporated to the films is negligible and the oxides are almost stoichiometric, the intensity of the luminescence emission is also negligible or zero. If, starting from this region, R is increased at a constant T to incorporate more Si to the layers, I increases progressively as the excess of Si does and reaches its maximum value, above 0.85, at the $(-1, +1, P)$ edge, where the excess of Si is around 0.2%. The absolute maximum, $I = 1$, is obtained at the $(-1, +1, -1)$ corner for a 0.22% of excess of Si. On the other hand, if T is increased keeping R constant to increment the excess of Si, I reaches only values near 0.7 in the proximity of the $(+1, -1, P)$ edge since too much Si in excess, up to 2.5%, has been incorporated as a result of the increase in T. If both T and R are increased simultaneously, the excess of Si increases steeply and I first increases slightly and then starts to decrease reaching very small values, $I \approx 0.2$, near the $(+1, +1, P)$ edge, where the excess of Si is greater than 50% for all values of P. In these samples, large Si clusters are expected to precipitate.

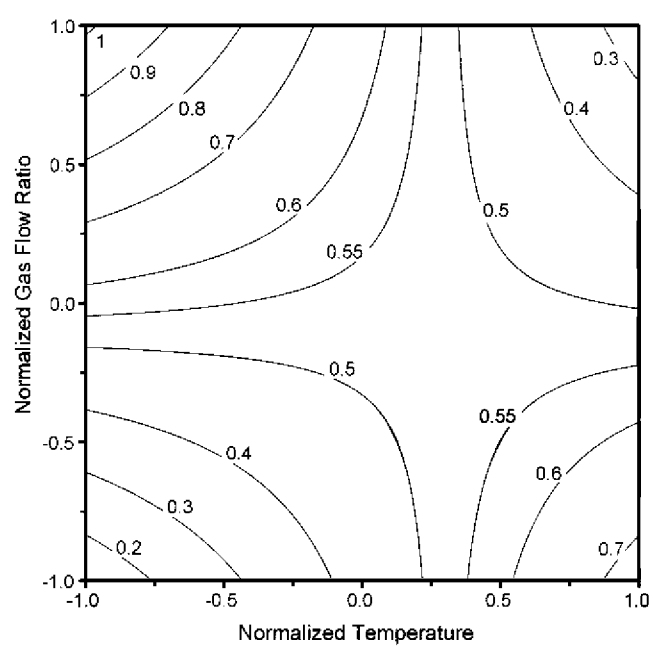

Fig. 6. Normalized intensity, I (a.u.), of the luminescence band at 665 nm as a function of the normalized values of T and R at $P = -1$.

Looking at Fig. 3, it is clear that there exist other combinations of values of the variables that could yield an excess of Si of 0.22%. The experimental results show that E value at (0, −1, 0) is ≈0.29% while $I \approx 0.5$ at this point. In the same way, at the centre of the (−1, R, P) face, the intensity is $I \approx 0.4$ with $E \approx 0.2\%$. These results suggest that the intensity of the luminescence band depends not only on the amount of Si in excess in the as-deposited sample, but also on the experimental conditions used to obtain it. In this case, the sample that yields the maximum intensity was deposited at the lowest temperature (250 °C), with a gas mixture as rich as possible in the precursor of Si (gas flow ratio $Si_2H_6/O_2 = 5$) and at the lowest total pressure (185 mTorr), although the influence of this last variable has not been critical. In these conditions the growth rate was below 40 nm/h.

The CL spectra of the samples measured at *RT* show only the 655 nm band, with an intensity around ten times lower than at 80 K, while the broad band at 570 nm does not appear.

4. Conclusions

Non-stoichiometric Si oxides have been deposited by LPCVD (with growth rates in the 15–60 nm/h range and excesses of Si from 0 to almost 70% in volume) using a FCCD experiment. The presence of Si–H bonds and the shift of the characteristic peaks of SiO_2 in the FTIR spectra are qualitative indications of the non-stoichiometry of the as-deposited oxides. Si nanoparticles embedded in SiO_2 have been synthesized by thermal annealing of the as-deposited samples at 1100 °C. These structures exhibit luminescence peaking at 665 nm associated to the Si nanoparticles at 80 K and at room temperature. A subsequent annealing at 450 °C in forming gas improves the intensity of the emission band by around 30%. The results of the FCCD show that the intensity of the band depends on the excess of Si incorporated to the films as well as on the combination of variables selected to get it, reaching a maximum for a value of the excess of Si of 0.22% obtained at low temperature, with a high Si_2H_6/O_2 flow ratio and at low pressure.

References

J.R. Aguilar, G. Monroy, M. Cárdenas, G.S. Contreras, Mater. Sci. Eng. C 27 (2007) 1074.

G.G. Ross, D. Barba, C. Dahmoune, Y.Q. Wang, F. Martin, Nucl. Instrum. Methods B 256 (2007) 211.

D.C. Montgomery, Design and Analysis of Experiments, John Wiley & Sons, New York, 2001.

M.I. Ortiz, J. Sangrador, A. Rodríguez, T. Rodríguez, A. Kling, N. Franco, N.P. Barradas, C. Ballesteros, Phys. Status Solidi (a) 203 (2006) 1284, and references therein.

M.J. Anderson, P.J. Whitcomb, RSM Simplified, Productivity Press, New York, 2004.

http://www.statease.com/.

E.D. Palik (Ed.), Handbook of Optical Constants of Solids, Academic, San Diego, CA, 1998.

J.C.G. de Sande, R. Serna, J. Gonzalo, C.N. Afonso, D.E. Hole, A. Naudon, J. Appl. Phys. 91 (2002) 1536.

H. Rinnert, M. Vergnat, G. Marchal, A. Burneau, Appl. Phys. Lett. 72 (1998) 3157.

X. Wu, Ch. Ossadnik, Ch. Eggs, S. Veprek, F. Phillipp, J. Vac. Sci. Technol. B 20 (2002) 1368.

H. Nishikawa, E. Watanabe, D. Ito, Y. Sakurai, K. Nagasawa, Y. Ohki, J. Appl. Phys. 80 (1996) 3513.